INTERNATIONAL JOURNAL OF
NUMERICAL ANALYSIS AND MODELING
Volume 16, Number 4, Pages 668–679

COLOR-TO-GRAY CONVERSION WITH PERCEPTUAL PRESERVATION AND DARK CHANNEL PRIOR

JUN LIU[1], FAMING FANG[2], AND NING DU[1]

Abstract. This paper aims to present a decolorization strategy based on perceptual consistency and dark channel prior. The proposed model consists of effective fidelity terms and a prior term. We use the ℓ_0-norm to control the sparsity of the dark channel prior. To solve the non-convex minimization problem, we employ the split and penalty technique to simplify the minimization problem and then solve it by the carefully designed iteration scheme. Besides, we show the convergence of the algorithm using Kurdyka-Łojasiewicz property. The numerical evaluation in comparison with other state-of-the-art methods demonstrates the effectiveness of the proposed method.

Key words. Color-to-gray, perceptual consistency, dark channel, Kurdyka-Łojasiewicz property, non-convex.

1. Introduction

Color-to-gray, which is also named as decolorization, is a technique that transforms a color image (3-D) to a grayscale one (1-D). It is of great importance in black-and-white printing, E-ink monotone display, image preprocessing (then for segmentation, edge detection) and object recognition. A natural problem in decolorization is that information loss happens due to dimension reduction. How to produce a perceptually plausible grayscale image, which hopes to preserve enough structures and contrast from the original color image, is the main concern in the literature. The application-driven tasks and unavoidable difficulties in decolorization make the problem important and attract a lot of research attention [6, 16, 15, 8].

Extracting the luminance channel in a transformed color space such as CIE Lab is an intuitive way of generating a grayscale image. Although this method is very simple and cost-less, it fails to preserve salient structures and features of the iso-luminant regions in the color images. Another simple decolorization method is to implement a linear combination of different channels if the color image is represented in RGB color space. The same disadvantage happens since the linear combination of different sets of R, G and B values may generate the same luminance response in the grayscale result [22]. To overcome this problem, many outstanding decolorization methods have been proposed to perceptually preserve salient features in the color-to-gray conversion.

As reported in [17, 11, 15, 14], decolorization methods can be roughly classified into two categories: one is the local mapping method which treats the pixels differently in different local regions in one image [2, 20, 11]; However, these algorithms would bring artifacts since they tried to visualize all details. The other type of

Received by the editors June 9, 2018, and in revised form, November 15, 2018.
2000 *Mathematics Subject Classification.* 65K10, 68U10, 68W40, 90C26.

method is the global mapping method which processes the pixel mapping independent of the pixel location [8, 9, 12, 21, 16]. Recently, deep learning based methods are used for decolorization. Zhang and Liu [27] proposed to combine global features and local semantic features learned by the convolution neural network for decolorization. They reported that their method can better preserve the contrast in both local color blocks and adjacent pixels of the color image. Cai et al. [7] proposed a system which used deep representations to extract content information based on human visual perception, and automatically selected suitable grayscale for decolorization.

Different from other methods, You et al. [25] emphasized that many existing methods mainly focus on best-preserving contrast while paying less attention to the consistency with human perception. The authors designed two optimization framework using ℓ_1-norm and ℓ_2-norm respectively. Their experiments showed that ℓ_1-norm works better than ℓ_2-norm. As we know, the computation related to ℓ_1 is more difficult compared with ℓ_2-norm. In this paper, we propose a new color to gray conversion model in light of the perceptual consistency and the dark channel prior. Our idea is to consider ℓ_1-norm and ℓ_2-norm in one model which can balance the quality and computation. Furthermore, to better improve the quality of decolorization, we enforce the sparsity prior to the dark channel. This prior has been successfully applied in blind deconvolution [19] and image dehazing [10]. Our experiments show that the proposed method works very well compared with other popular decolorization methods.

The main contribution of this paper is that we propose a new sparsity-driven and perceptually consistent model for decolorization. The perceptual fidelity on brightness and contrast are controlled by the ℓ_1 norm and the ℓ_2 norm, respectively. The prior information of the gray is that the dark channel property preservation. To control the sparsity the dark channel, we use ℓ_0 norm as a regularization term. We propose an alternating minimization algorithm with the technique of split and penalty to solve our model. Although the ℓ_0-norm which makes the problem highly nonconvex, we use Kurdyka-Łojasiewicz (KL) property [4] to prove the convergence of the related algorithm.

2. Proposed method

2.1. Related work. In [25], You et al. elaborately proposed a graphical model based method which balances brightness and contrast perceptual consistency. They aim to preserve the perceptual properties of the color image as much as possible. The model is composed of the brightness perceptual energy E_b and the contrast consistency term E_c:

$$E_b(g) = \|\Lambda(p_1 - g)\|_\ell,\ E_c(g) = \sum\nolimits_{i=1}^{3} \alpha_i \|C(p_i - g)\|_\ell, \tag{1}$$

where $g \in \mathbb{R}^{mn\times 1}, p_i \in \mathbb{R}^{mn\times 1}, i = 1, 2, 3$, m and n are the height and width of the input image. g is the decolorized gray-scale image, p_1 is the brightness, p_2 and p_3 are the color values in the CIE Lab space of the input color image, respectively. The parameters $\alpha_i, i = 1, 2, 3$ balance the importance between different channels.

The diagonal matrix $\Lambda \in \mathbb{R}^{mn\times mn}$ is with $\Lambda_{i,i} = \frac{1}{(\sqrt{100^2-{p_2}^2-p_3^2+\epsilon})_i(\sqrt{100^2-(2p_1-100)^2+\epsilon})_i}$, where ϵ is a small positive constant. Note that $\Lambda_{i,i}$ is used to penalize color with large variance. The matrix C is the complex contrast operator constructed from several linear combination of difference of Gaussian kernel. In [25], the authors pointed out that the model had closed-form solution when $\ell = 2$. While for $\ell = 1$, the iteratively reweighted least square method is used to find the solution. For the details of matrices Λ and C, please check You et al's work [25].

2.2. Proposed model. In this section, we propose a new color-to-gray conversion method by using both ℓ_1 norm and ℓ_2 norm based on You et al.'s work [25]. This modification can balance the simplicity of computation and the quality of decolorization. More importantly, we incorporate a regularization function: the dark channel prior. This term describes the minimum values in an image patch and has been successfully applied in image dehazing [10] and image blind deconvolution [19]. The reason we employ this prior is that most elements of the dark channel are zero for natural color images. This prior is used to restrict the minimization of a pixel value on the local region of the image. In a small local neighborhood, the smaller dark channel value is, the more obvious contrast is and vice versa. We want to keep this property after the color-to-gray conversion.

Based on You et al's perceptual measurement method and the dark channel prior, our model is proposed as follows:

$$\min_g \|\Lambda(g-p_1)\|_1 + \sum_{i=1}^{3} \alpha_i \|C(g-p_i)\|_2^2 + \eta \|D(g)\|_0, \tag{2}$$

where the dark channel $D(g)(x) = \min_{y\in\mathcal{N}(x)} \mathbf{g}(y)$, x and y are the pixel locations of the gray image $\mathbf{g}$, where $\mathbf{g}$ is matrix version of g, $\mathcal{N}(x)$ is an image patch centered at x. Although the operator $D(\cdot)$ is a non-linear function, as observed in [19], the non-linear operation $D(g)$ is equivalent to a linear operator M multiply g. The matrix M is computed by

$$M(x,z) = \begin{cases} 1, & z = \arg\min_{u\in\mathcal{N}(x)} \mathbf{g}(u), \\ 0, & \text{otherwise.} \end{cases} \tag{3}$$

Then the minimization problem (2) can be rewritten as:

$$\min_g \|\Lambda(g-p_1)\|_1 + \sum_{i=1}^{3} \alpha_i \|C(g-p_i)\|_2^2 + \eta \|Mg\|_0. \tag{4}$$

The advantages of the proposed model are: 1) perceptually driven brightness and contrast consistency; 2) dark channel property preservation.

2.3. Algorithm. We use the split and penalty technique to design alternating scheme to solve the corresponding minimization problem. By introducing two auxiliary variables f and v, we transform the unconstrained problem (4) into the following equivalent constrained problem:

$$\begin{aligned} &\min_{g,f,w} \|\Lambda(f-p_1)\|_1 + \sum\nolimits_{i=1}^{3} \alpha_i \|C(g-p_i)\|_2^2 + \eta\|w\|_0, \\ &s.t.\ f = g,\ Mg = w. \end{aligned} \tag{5}$$

Using the penalty technique, we set problem (5) as

$$\min_{g,f,w} \|\Lambda(f-p_1)\|_1 + \sum\nolimits_{i=1}^{3} \alpha_i \|C(g-p_i)\|_2^2 + \eta\|w\|_0 + \gamma\|Mg-w\|_2^2 + \beta\|f-g\|_2^2. \tag{6}$$

This formulation benefits the algorithm design so that we can solve (6) efficiently. We can alternatively minimize the function with respect to one variable while other variables are temporarily fixed. To ensure the convergence of the algorithm, we carefully design the following iteration scheme:

Given g^k, f^k and w^k, the minimizer w^{k+1} can be obtained by solving

$$w^{k+1} = \arg\min_{w} \gamma\|w - Mg^k\|_2^2 + \eta\|w\|_0 + \sigma_1\|w - w^k\|_2^2. \tag{7}$$

The solution is given by a shrinkage [24],

$$w^{k+1} = \begin{cases} Mg^k, & \gamma|Mg^k|^2 + \sigma_1|w^k|^2 \geq \eta, \\ 0, & \text{otherwise.} \end{cases} \tag{8}$$

For the subproblem of g given f^k and w^{k+1},

$$g^{k+1} = \arg\min_{g} \sum\nolimits_{i=1}^{3} \alpha_i \|C(g-p_i)\|_2^2 + \gamma\|Mg - w^{k+1}\|_2^2 + \beta\|f^k - g\|_2^2. \tag{9}$$

This linear least squares minimization problem has unique solution given by solving its normal equations:

$$(\beta + \sum\nolimits_{i=1}^{3} \alpha_i C^T C + \gamma M^T M) g^{k+1} = \beta f^k + M^T w^{k+1} + C^T C \sum\nolimits_{i=1}^{3} \alpha_i p_i. \tag{10}$$

Note that $M^T M$ is identity operator (please see the supplemental material of [19] for detail [18]), $C^T C$ has block circulant with circulant blocks (BCCB) structure when the periodic boundary conditions are used. Then the computation is very efficient by the discrete Fourier transformations (DFTs) [28, 23].

Given g^{k+1} and w, we solve f^{k+1} by

$$f^{k+1} = \arg\min_{f} \|\Lambda(f-p_1)\|_1 + \beta\|f - g^{k+1}\|_2^2 + \sigma_2\|f - f^k\|_2^2. \tag{11}$$

It is a simple shrinkage computation [13], i.e.,

$$f^{k+1} = \max\left\{ \frac{|\xi^k|}{2(\beta+\sigma_2)} - \frac{\Lambda \mathbb{1}}{2(\beta+\sigma_2)}, 0 \right\} \cdot \operatorname{sign}(\xi^k) + p_1, \tag{12}$$

where $\xi^k = \beta(g^{k+1} - p_1) + \sigma_2(f^k - p_1)$ and $\mathbb{1}$ denotes a vector with each element equals 1.

Above all, we summarize the iteration scheme for solving the minimization problem (6) as Algorithm 1 shown below:

Algorithm 1 Alternating iteration for solving minimization problem (6)

1. ***initialization:*** given (f^0, g^0)
2. ***iteration:*** generate a sequence $\{(w^k, g^k, f^k)\}$
   1) *solve for* w^{k+1} *using* (8)*;*
   2) *solve for* g^{k+1} *using* (10)*;*
   3) *solve for* f^{k+1} *using* (12).
3. ***stop:*** if a stopping criterion is satisfied

Definition 1. (*KL property* [1, 26]) Let $\sigma : \mathbb{R}^d \to (-\infty, +\infty]$ be a proper lower semicontinuous function.

1) For $\bar{x} \in \text{dom}\ \partial\sigma := \{x \in \mathbb{R}^d : \partial\sigma(x) \neq \varnothing\}$, if there exists an $\eta \in (0, +\infty]$, a neighborhood X of $\bar{x}$ and a function $\xi \in \Phi_\eta$, such that for all $x \in X \cap \{\sigma(\bar{x} < \sigma(x) < \sigma(\bar{x}) + \eta)\}$, the following inequality holds

$$\phi'(\sigma(u) - \sigma(\bar{x}))\text{dist}(0, \partial\sigma(x)) \geq 1,$$

then σ is said to have the Kurdyka-Łojasiewicz (KL) property at $\bar{x}$. Note that Φ_η denotes the class of all concave and continuous functions $\xi : [0, \eta) \to \mathbb{R}_+, \eta \in \mathbb{R}_+$ which satisfies: *a)* $\xi(0) = 0$; *b)* ξ is continuous differentiable on $(0, \eta)$; *c)* for all $s \in (0, \eta)$, $\xi'(s) > 0$.

2) σ is called a KL function, if σ satisfies the KL property at each point of dom $\partial\sigma$.

Theorem 1. *Let* $\{\nu^k = (w^k, g^k, f^k)\}_{k\in\mathbb{N}}$ *be a sequence generated by Algorithm 1, then* $\{\nu^k\}$ *converges to* ν^* *which is a critical point of* (6).

Proof. For the convenience of theoretical analysis, we set

$$\Phi(w, g, f) = H(w, g, f) + \phi_1(w) + \phi_2(f), \tag{13}$$

where $H(w, g, f) = \sum_{i=1}^3 \alpha_i \|C(g - p_i)\|_2^2 + \gamma\|Mg - w\|_2^2 + \beta\|f - g\|_2^2$, $\phi_1(w) = \eta\|w\|_0$ and $\phi_2(f) = \|\Lambda(f - p_1)\|_1$. Let the sequence $\nu^k = \{(w^k, g^k, f^k)\}$, and $\partial\Phi(\nu^k) = (\partial_w\Phi(\nu^k), \partial_g\Phi(\nu^k), \partial_f\Phi(\nu^k))$. Then we have

$$\partial_w\Phi(\nu^{k+1}) = 2\gamma(w^{k+1} - Mg^{k+1}) + \eta\partial_w\phi_1(w^{k+1}); \tag{14}$$

$$\partial_g\Phi(\nu^{k+1}) = 2\sum_{i=1}^3 \alpha_i C^T C(g^{k+1} - p_i) + 2\gamma M^T(Mg^{k+1} - w^{k+1}); \tag{15}$$

$$\partial_f\Phi(\nu^{k+1}) = 2\beta(f^{k+1} - g^{k+1}) + \Lambda^T\partial_f\phi_2(f^{k+1}). \tag{16}$$

According to Algorithm 1 and equations (14)-(16), we obtain

$$\partial_w\Phi(\nu^{k+1}) = 2\gamma M(g^k - g^{k+1}) - 2\sigma_1(w^{k+1} - w^k); \tag{17}$$

$$\partial_g\Phi(\nu^{k+1}) = 2\beta(f^k - f^{k+1}); \tag{18}$$

$$\partial_f\Phi(\nu^{k+1}) = 2\sigma_2(f^{k+1} - f^k). \tag{19}$$

i.e., a subgradient lower bound for the iterates gap satisfies

$$\begin{aligned}\|\partial\Phi(\nu^{k+1})\|_2 \leq\ & 2\gamma\|M\|_F\|g^k - g^{k+1}\|_2 + 2\sigma_1\|w^k - w^{k+1}\|_2 \\ & + 2(\sigma_2 + \beta)\|f^k - f^{k+1}\|_2 \leq \rho_1\|\nu^k - \nu^{k+1}\|_2,\end{aligned} \tag{20}$$

where $\rho_1 = 2\max\{\gamma\|M\|_F, \sigma_1, \sigma_2 + \beta\}$.

Then we will next prove the sufficient decrease property for the iterates gap. It is easy to check

$$\Phi(w^k, g^k, f^k) - \Phi(w^{k+1}, g^k, f^k) \geq 2\sigma_1 \|w^k - w^{k+1}\|_2^2. \tag{21}$$

For g-subproblem, using Taylor expansion g^{k+1} of Φ, we know that

$$\Phi(w^{k+1}, g^k, f^k) - \Phi(w^{k+1}, g^{k+1}, f^k) \geq 2\beta \|g^k - g^{k+1}\|_2^2. \tag{22}$$

Since f^{k+1} is the stationary point of f-subproblem, we get

$$\Phi(w^{k+1}, g^{k+1}, f^k) - \Phi(w^{k+1}, g^{k+1}, f^{k+1}) \geq 2\sigma_2 \|f^k - f^{k+1}\|_2^2. \tag{23}$$

Summing up (21), (22) and (23), we obtain the sufficient decrease property

$$\Phi(w^k, g^k, f^k) - \Phi(w^{k+1}, g^{k+1}, f^{k+1}) \geq 2\rho_2 \|\nu^k - \nu^{k+1}\|_2^2, \tag{24}$$

where $\rho_2 = 2\min\{\sigma_1, \sigma_2, \beta\}$.

We will next prove Theorem 1 using KL inequality. In Jacek et al's monograph [3], the Euclidean norm $\|\cdot\|$ is shown to be semi-algebraic. Furthermore, $\|\cdot\|_1$-norm and $\|\cdot\|_0$-norm are also shown to be semi-algebraic [4]. Thus, we know Φ is semi-algebraic and then satisfies the KL property an any point of dom(Φ) according to Theorem 3 in [4]. Then by Theorem 1 in [4], we know that the sequence $\{\nu^k\}_{k\in\mathbb{N}}$ converges to a critical point $\nu^* = (w^*, g^*, f^*)$ of Φ. The proof completes. □

As we know, as $\beta, \gamma \to \infty$, the solution of (6) converges to that of (4). In real application, we intuitively set a gradual incrementation on the penalty parameter β and γ. The corresponding algorithm is shown as follows:

Algorithm 2 Decolorization by perceptual consistence and dark channel prior

1. ***initialization:*** given (f^0, g^0), *the maximum penalty value* P_{max}
2. ***iteration:*** generate a sequence $\{(w^k, g^k, f^k)\}$

while $\beta < P_{max}$, *Do*

1) *solve for* w^{k+1} *using* (8);
2) *solve for* g^{k+1} *using* (10);
3) *solve for* f^{k+1} *using* (12);
4) *update* $\beta = 2 * \beta$, $\gamma = 2 * \gamma$.

3. Numerical experiments

In this section, we present numerical results to illustrate the performance of our method. We compare the proposed method with state-of-the-art methods [16, 15, 14, 11]. The test color images are from Cadik's color-to-gray benchmark dataset which is publicly available [5]. The quantitative evaluation for different methods is the average color contrast-preserving ratio (ACCPR) [16]. The results by Lu et al. [16] and Smith [20] can be obtained from `http://www.cse.cuhk.edu.hk/~leojia/projects/color2gray/` and `http://cadik.posvete.cz/color_to_gray_evaluation/`. For the results obtained by Jin et al. [11] and Liu et al. [15, 14], we use the suggested parameters in their codes which can be downloaded from the authors' homepage to get the best results. For our method, we fix the parameters $\sigma_1 = \sigma_2 = 1 \times 10^{-3}$, $\alpha_2 = \alpha_3, \beta_0 = \gamma_0 = 2 * \eta$, $P_{max} = 2^6$ and tune the α_1, α_2 and η empirically to get the best visual and quantity performance.

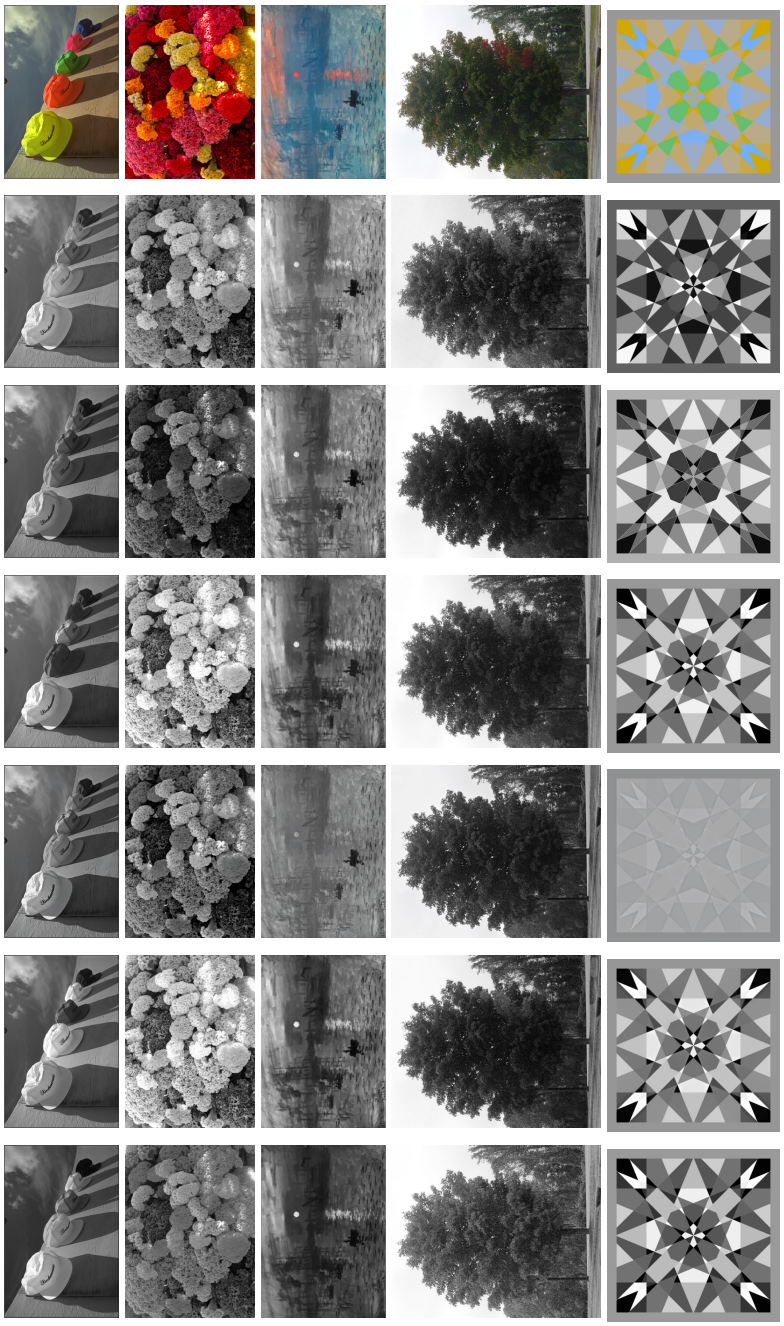

(a) Lu et al. [16] (b) Jin et al. [11] (c) Smith et al. [20] (d) Liu et al. [15] (e) Liu et al. [14] (f) Ours (g) color

FIGURE 1. Decolorization comparison by different methods.

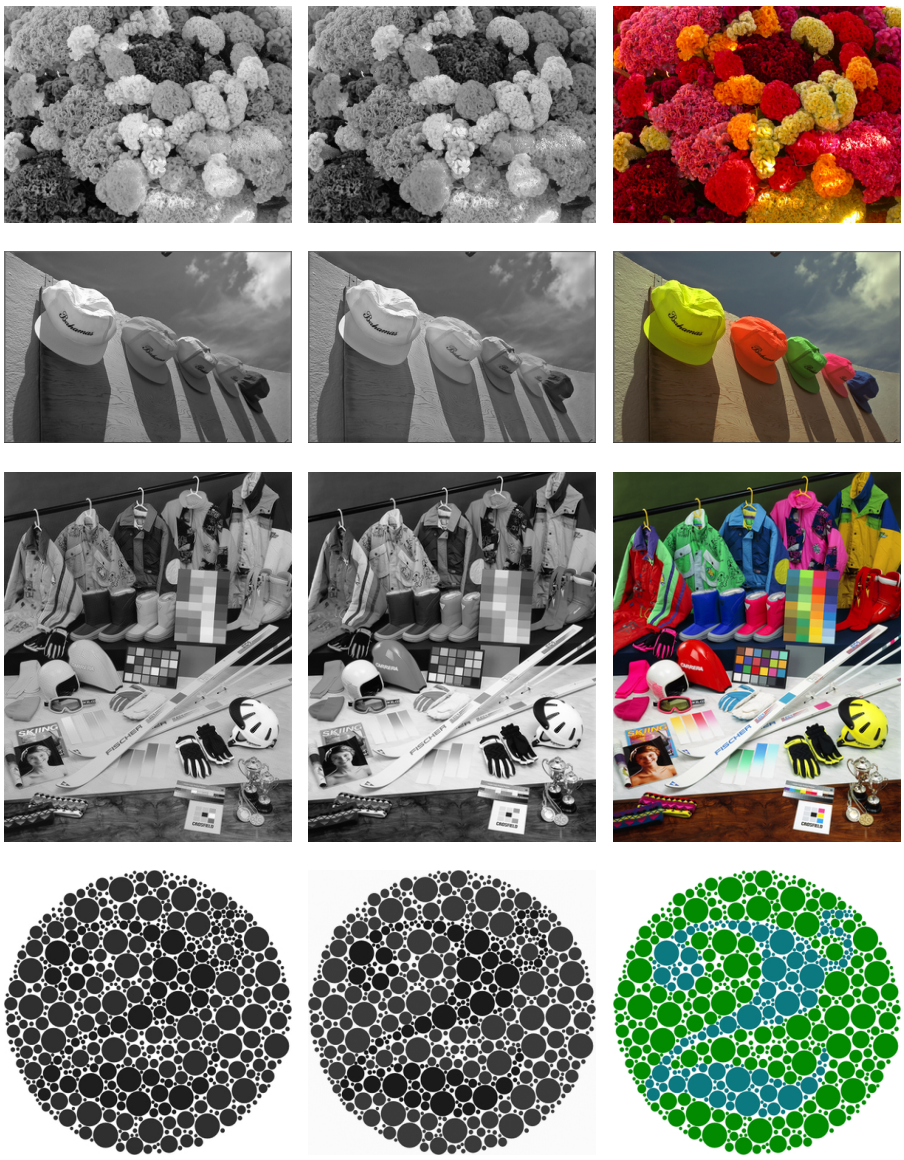

(j) without dark-prior (k) with dark-prior (l) color

FIGURE 2. The decolorization results by our method without the dark channel prior and with the dark channel prior.

In Table 1, we report the ACCPR values for decolorization of all test images in the dataset. According to the table, we observe that our method gives the highest value for eight images and Liu's gradient correlation similarity method [15] gives the highest value for six images. In total, our method performs better than the

other methods, in terms of the average ACCPR value. Due to the limited space of this paper, we only present three representative images decolorized by different methods. The decolorized images and color images are shown in Fig. 1. From the figures, we observe that our decolorized results can keep the color contrast and luminance better than other methods. Specifically, according to the color conversion of the sunlight and flower color, our method can perceptually reflect the color distinctiveness and preserve the contrast better than the methods of Jin et al. [11] and Liu et al. [14]. Note that Lu et al.'s method gives the result with incorrect contrast, i.e., it is too dark compared with the color image. Although Liu et al.'s method [15] performs better than the methods in [16, 11, 20], it is not that good in comparison with our result and the method in [14] which can be seen from the boats in decolorized images. In the third row of Fig. 1, we can observe that the result obtained by our method can perceptually preserve the contrast and brightness of the color image compared with other methods.

TABLE 1. The ACCPRs of the decolorized images in the dataset by different methods. The boldface number refers to the largest value in each row.

Image	Lu[16]	Jin[11]	Liu[14]	Liu[15]	ours
1	0.5465	0.5294	0.5148	**0.5858**	0.4841
2	0.9792	0.9705	0.9694	0.9678	**0.9858**
3	0.7722	0.7476	0.7740	**0.8206**	0.6004
4	0.5398	0.6003	0.5190	0.5907	**0.7976**
5	0.7628	**0.7998**	0.7568	0.7604	0.5613
6	0.5985	0.5865	0.5237	0.5839	**0.7372**
7	**0.9261**	0.8952	0.7718	0.6403	0.8250
8	0.6729	0.6204	**0.7154**	0.6465	0.5818
9	0.4167	0.6962	0.4672	**0.7005**	0.5900
10	0.5674	0.6121	0.6161	**0.6749**	0.5926
11	0.8461	0.7580	**0.8661**	0.7945	0.7541
12	0.7110	0.6836	0.5383	0.6034	**0.8854**
13	0.2677	0.4104	0.4038	0.4024	**0.7699**
14	0.6078	**0.7654**	0.7388	0.7286	0.4457
15	**0.7074**	0.6847	0.6815	0.6395	0.6441
16	0.7127	0.6732	0.6645	**0.7288**	0.7157
17	0.8069	0.8113	**0.9588**	0.6882	0.6554
18	0.5288	0.5887	0.6381	0.6876	**0.8777**
19	0.5458	0.7197	0.6537	**0.7201**	0.6848
20	0.4776	0.7075	**0.7213**	0.6839	0.7087
21	0.9252	**0.9596**	0.9585	0.9562	0.6387
22	0.7155	0.5425	0.4752	0.5295	**0.9462**
23	**0.7431**	0.4342	0.5949	0.5736	0.6340
24	0.8274	0.7816	0.6765	0.7832	**0.8555**
Avg	0.6752	0.6908	0.6749	0.6871	**0.7071**

We also show the decolorization results by our model with the dark channel prior and without dark channel prior in Fig. 2. As shown in the figures, we can observe that both methods can generate good color-to-gray conversion results while our model with the dark channel prior can better distinguish the contrast of the test color images.

Since the code is not available for the method of You et al. [25], we do not evaluate the ACCPR result here and we only compare the visual quality of decolorization results. The decolorized images of You et al.'s method are directly cropped from the authors' paper. As can be seen from Fig. 3, both methods can preserve the contrast and brightness of the original color images. The decolorization results obtained by our method is slightly better than You et al.'s method.

4. Conclusion

In this paper, we have presented an effective decolorization method based on perceptual preservation and the dark-channel prior. Our model can perceptually keep the contrast and brightness of the color image. Besides, we carefully design the iteration algorithm and prove the corresponding convergence property. Numerical results on a publicly available test dataset show that our method is competitive with some other state-of-the-art methods.

Disclosures. The authors declare there is no relevant financial interests and no potential conflicts of interest regarding the publication of this paper.

Acknowledgments

This research was supported by NSFC (11631003, 1690012, 11701079, 61501188), This paper was supported by the Jilin Provincial Science and Technology Development Plan funded project (20170520050JH,20170520053JH), Fundamental Research Funds for the Central Universities (2412016KJ013) and China Postdoctoral Science Foundation (2016M601360).

References

[1] H. Attouch and J. Bolte. On the convergence of the proximal algorithm for nonsmooth functions involving analytic features. *Mathematical Programming*, 116(1):5–16, 2009.

[2] R. Bala and R. Eschbach. Spatial color-to-grayscale transform preserving chrominance edge information. In *Color and Imaging Conference*, pages 82–86, 2004.

[3] J. Bochnak, M. Coste, and M.-F. Roy. *Real Algebraic Geometry*. Springer Berlin Heidelberg, 1998.

[4] J. Bolte, S. Sabach, and M. Teboulle. Proximal alternating linearized minimization for nonconvex and nonsmooth problems. *Mathematical Programming*, 146(1-2):459–494, 2014.

[5] M. Čadík. Perceptual evaluation of Color-to-Grayscale image conversions. In `http://cadik.posvete.cz/color_to_gray_evaluation/`.

[6] M. Čadík. Perceptual evaluation of Color-to-Grayscale image conversions. *Computer Graphics Forum*, 27(7):1745–1754, 2008.

[7] B. Cai, X. Xu, and X. Xing. Perception preserving decolorization. *IEEE International Conference on Image Processing*, 2018.

[8] A. A. Gooch, S. C. Olsen, J. Tumblin, and B. Gooch. Color2gray: salience-preserving color removal. In *ACM SIGGRAPH*, pages 634–639, 2005.

[9] M. Grundland and N. A. Dodgson. Decolorize: Fast, contrast enhancing, color to grayscale conversion. *Pattern Recognition*, 40(11):2891–2896, 2007.

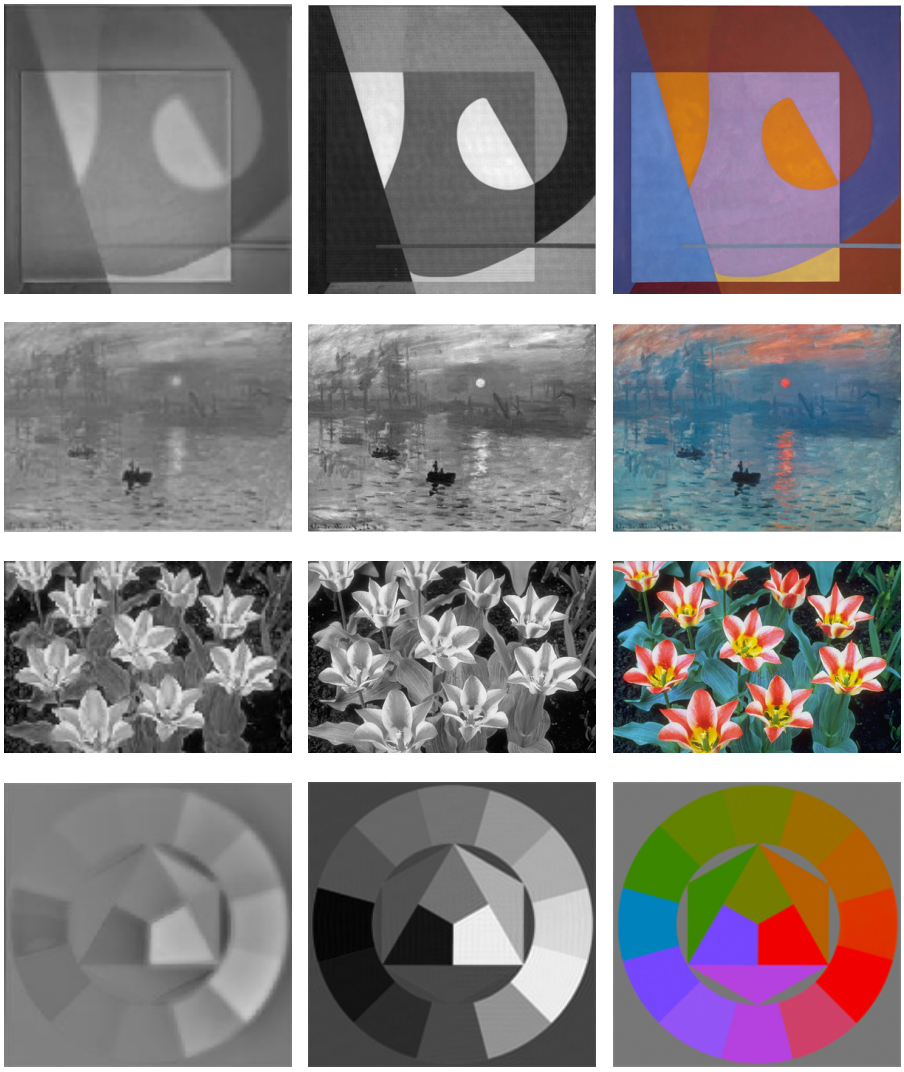

(j) You et al.'s (k) Ours (l) Color image

FIGURE 3. The decolorization results by our method and You et al.'s method [25].

[10] K. He, J. Sun, and X. Tang. Single image haze removal using dark channel prior. *Pattern Analysis and Machine Intelligence, IEEE Transactions on*, 33(12):2341, 2011.

[11] Z. Jin, F. Li, and M. K. Ng. A variational approach for image decolorization by variance maximization. *SIAM Journal on Imaging Sciences*, 7(2):944–968, 2014.

[12] J. G. Kuk, J. H. Ahn, and N. I. Cho. A color to grayscale conversion considering local and global contrast. In *Asian Conference on Computer Vision*, pages 513–524, 2010.

[13] J. Liu, T. Z. Huang, X. G. Lv, and J. Huang. Restoration of blurred color images with impulse noise. *Computers & Mathematics with Applications*, 70(6):1255–1265, 2015.

[14] Q. Liu, P. X. Liu, Y. Wang, and H. Leung. Semiparametric decolorization with laplacian-based perceptual quality metric. *IEEE Transactions on Circuits & Systems for Video Technology*, 27(9):1856–1868, 2017.

[15] Q. Liu, P. X. Liu, W. Xie, Y. Wang, and D. Liang. Gcsdecolor: Gradient correlation similarity for efficient contrast preserving decolorization. *IEEE Transactions on Image Processing*, 24(9):2889–2904, 2015.

[16] C. Lu, L. Xu, and J. Jia. Contrast preserving decolorization. In *IEEE International Conference on Computational Photography*, pages 1–7, 2012.

[17] C. Lu, L. Xu, and J. Jia. Real-time contrast preserving decolorization. In *SIGGRAPH Asia 2012 Technical Briefs*, page 34. ACM, 2012.

[18] J. Pan, D. Sun, H. Pfister, and M.-H. Yang. Blind image deblurring using dark channel prior supplemental material. In *http://vllab1.ucmerced.edu/~jinshan/projects/dark-channel-deblur/*.

[19] J. Pan, D. Sun, H. Pfister, and M.-H. Yang. Blind image deblurring using dark channel prior. In *Proceedings of the IEEE Conference on Computer Vision and Pattern Recognition*, pages 1628–1636, 2016.

[20] K. Smith, P. Landes, J. Thollot, and K. Myszkowski. Apparent greyscale: A simple and fast conversion to perceptually accurate images and video. *Computer Graphics Forum*, 27(2):193–200, 2008.

[21] M. Song, D. Tao, C. Chen, X. Li, and C. W. Chen. Color to gray: Visual cue preservation. *IEEE Transactions on Pattern Analysis and Machine Intelligence*, 32(9):1537–1552, 2010.

[22] Y. Song, L. Bao, X. Xu, and Q. Yang. Decolorization: is rgb2gray() out? In *SIGGRAPH Asia 2013 Technical Briefs*, pages 1–4, 2013.

[23] C. Wu and X. Tai. Augmented lagrangian method, dual methods, and split bregman iteration for rof, vectorial tv, and high order models. *SIAM Journal on Imaging Sciences*, 3(3):300–339, 2010.

[24] L. Xu, C. Lu, Y. Xu, and J. Jia. Image smoothing via L0 gradient minimization. In *Proceedings of the 2011 SIGGRAPH Asia Conference*, volume 20, pages 174:1–174:12, 2011.

[25] S. You, N. Barnes, and J. Walker. Perceptually consistent color-to-gray image conversion. *arXiv preprint arXiv:1605.01843*, 2016.

[26] X. Zhang, M. Bai, and M. K. Ng. Nonconvex-TV based image restoration with impulse noise removal. *SIAM Journal on Imaging Sciences*, 10(3):1627–1667, 2017.

[27] X. Zhang and S. Liu. Contrast preserving image decolorization combining global features and local semantic features. *The Visual Computer*, 34(6):1099–1108, 2018.

[28] X. Zhao, W. Wang, T. Zeng, T. Huang, and M. Ng. Total variation structured total least squares method for image restoration. *SIAM Journal on Scientific Computing*, 35(6):B1304–B1320, 2013.

School of Mathematics and Statistics/Key Laboratory of Applied Statistics of MOE, Northeast Normal University, Changchun, PR China, 130024
E-mail: liuj292@nenu.edu.cn

Department of Computer Science, East China Normal University, Shanghai, PR China, 201101
E-mail: fmfang@cs.ecnu.edu.cn

School of Mathematics and Statistics/Key Laboratory of Applied Statistics of MOE, Northeast Normal University, Changchun, PR China, 130024
E-mail: dun933@nenu.edu.cn